Published in final edited form as:
J Immunol. 2012 July 1; 189(1): 425–432. doi:10.4049/jimmunol.1200063.

CD8+ T Cells Suppress Viral Replication in the Cornea but Contribute to VEGF-C Induced Lymphatic Vessel Genesis[1]

Christopher D. Conrady[*], **Min Zheng**[†], **Donald U. Stone**[†], and **Daniel J.J. Carr**[*,†,2]

[*]Department of Microbiology, Immunology, University of Oklahoma Health Sciences Center, Oklahoma City, OK 73104

[†]Department of Ophthalmology, University of Oklahoma Health Sciences Center, Oklahoma City, OK 73104

Abstract

HSV-1 is the leading cause of infectious corneal blindness in the industrialized world. $CD4^+$ T cells are thought to be the major leukocyte population mediating immunity to HSV-1 in the cornea as well as the likely source of immunopathology that reduces visual acuity. However, the role of $CD8^+$ T cells in immune surveillance of the cornea is unclear. Thus, we sought to evaluate the role of $CD8^+$ T cells in ocular immunity using transgenic mice in which greater than 98% of $CD8^+$ T cells are specific for the immunodominant HSV-1 epitope (gBT-I.1). We found in the cornea a significant reduction in virus, elevation in HSV-specific $CD8^+$ T cell influx, and more $CD8^+$ T cells expressing CXCR3 in transgenic mice compared to wild type (WT) controls yet similar acute corneal pathology. However by day 30 post infection, WT mice had drastically more blood and lymphatic vessel projections into the cornea compared to gBT-I.1 mice where only lymphatic vessel growth in response to vascular endothelial growth factor (VEGF)-C could be appreciated. Taken together, $CD8^+$ T cells are required to more efficiently eliminate virus from the cornea but play a minimal role in immunopathology as a source of VEGF-C.

INTRODUCTION

Herpes simplex virus type 1 (HSV-1) is a neurotropic, double-stranded DNA virus proven to be a highly successful pathogen based on seroconversion of the adult population in excess of 60% (1). The virus is spread through a mucocutaneous route, where it first invades host epithelium to eventually gain access to sensory nerve fibers. HSV-1 is then transported in a retrograde fashion to the cell body that populates sensory ganglia such as the trigeminal ganglia where the virus persists in a latent state (2). The virus can then sporadically reactivate in response to stressors (e.g. environmental stressors including UV exposure, temperature changes, and intellectual challenge) sending infectious virions down the maxillary or mandibular branch of the trigeminal nerve by anterograde transport to produce a lesion or “cold sore” on or near the labium. In stark contrast to labial lesions, more atypical presentations include primary or recurrent infection (reactivation) that induces significant yet devastating pathology in the CNS [i.e. encephalitis] (3) and cornea.

[1]This work was supported in part by NIH grant EY021238 to DJJC. Additional support includes P20 RR017703, an unrestricted grant from Research to Prevent Blindness and an OUHSC Presbyterian Health Foundation Presidential Professorship award to DJJC.

[2]Corresponding author: Daniel J.J. Carr, Ph.D., Department of Ophthalmology, DMEI #415, The University of Oklahoma Health Sciences Center, 608 Stanton L. Young Blvd., Oklahoma City, OK. 73104, Ph: (405) 271-8784, Fax: (405) 271-8128, dancarr@ouhsc.edu.

Disclosure
The authors do not have any conflicts of interest to declare and have all approved the final manuscript.

In the cornea, a site innervated by the ophthalmic division of the trigeminal nerve, HSV-1 can periodically reactivate to induce recurrent inflammatory conditions (4) in the stroma or epithelium known as epithelial or stromal keratitis (HSK),3 respectively. In the stroma the disease can progress to result in significant and permanent scarring and is the leading cause of infectious corneal blindness in the developed world (5). The cornea relies on transparency and proper shape to filter light to the lens and retina. Any alteration (i.e. inflammatory insults and scarring) to light passage in the eye can have drastic effects on visual acuity. Thus, understanding the immune response to HSV-1 in the cornea and the perpetual effects of these responses are critical in tailoring treatments to eradicate the virus while limiting permanent pathology severely affecting vision. Current experimental evidence implicates a vast portion of the pathology during HSK episodes is likely orchestrated by infiltrating neutrophils (6, 7) and $CD4^+$ T cells (8, 9). Reports have even shown that $CD4^+$ T cells localize to areas of keratitis (10).

Conversely, the $CD8^+$ T cell driven immune response is crucial in the containment of HSV-1 in tissues outside of the cornea (11, 12). Mice deficient in innate type I interferon (IFN) signaling (type I IFN receptor A1 or $CD118^{-/-}$) are extremely susceptible to rapid HSV-1 dissemination; however, when HSV-specific $CD8^+$ T cells are adoptively transferred into $CD118^{-/-}$ mice, recipients show a significant reduction in the viral load of the brain stem and trigeminal ganglia (13). These results highlight the importance of $CD8^+$ T cells in immune surveillance of HSV-1 in neuronal tissue but fail to address whether $CD8^+$ T cells are necessary to control HSV-1 replication in the cornea.

While several groups have attempted to describe the function of $CD8^+$ T cells in ocular immunity to HSV-1, they have failed to address a definitive role of $CD8^+$ T cells in clearing HSV-1 and/or inducing ocular pathology during the initial stages of infection. Models employing knockout mice for $CD4^+$ and $CD8^+$ T cell populations have been used to evaluate the specific roles of $CD4^+$ and $CD8^+$ T cells (9, 14–16). In terms of the role of $CD8^+$ T cells, two recent reports described the importance of a $CD4^+$ T cell influx regulating $CD8^+$ T cell entry into mucosal sites following infection (17) as well as an inherent role of $CD4^+$ T cells in priming $CD8^+$ T cells to attain competent IFN-γ and tumor necrosis factor-α production in response to HSV-1 (18). Consequently, abolishing $CD4^+$ T cells could hinder $CD8^+$ T cell access to the infected cornea as well as diminish their effector function clouding conclusions drawn from these studies. Relative to $CD8^+$ T cells in the presence of $CD4^+$ T lymphocytes, only two reports have evaluated viral replication during acute infection. One report measured viral shedding into the tear film and found no difference in mice with or without $CD8^+$ T cells (19). However, another group reported a rise in infectious virus in the periocular skin and tear film in the absence of $CD8^+$ T cells during acute infection (16). Based on the discrepancy in the literature on the role of $CD8^+$ T cells in viral surveillance within the cornea following infection, we initiated a study using mice in which greater than 98% of $CD8^+$ T cells are HSV-1 specific (20). These mice were previously found to be useful in establishing the importance of HSV-specific $CD8^+$ T cells in limiting virus egress in a cutaneous model of infection (21).

Thus, we hypothesized that $CD8^+$ T cells were critical in inhibiting viral replication in the cornea in response to HSV-1 infection while contributing to immune-mediated pathology that others have attributed to $CD4^+$ T cells. However, in the present study we found that while $CD8^+$ T cells actively participate in containing HSV-1 replication, their presence in the cornea was not associated with more severe pathology (i.e. matrix metalloproteinase-9

[3]Abbreviations used in this paper: WT, wild type; HSK, herpetic stromal keratitis; MLN, mandibular lymph node; gB, glycoprotein B; pi, post infection; IFN, interferon; MMP, matrix metalloproteinase; VEGF, vascular endothelial growth factor;

[MMP-9] expression and slit lamp examination) despite their contribution to the production of vascular endothelial growth factor (VEGF)-C and lymphangiogenesis.

MATERIALS AND METHODS

Mice and Virus

C57BL/6J wild type (WT) mice were purchased from the Jackson Laboratory (Bar Harbor, ME). HSV glycoprotein B (gB)T-I.1 T cell receptor (TCR) transgenic mice (20) on a WT background were maintained in the Dean McGee Eye Institute's animal facility and were all genotyped to confirm the presence of the transgene. gBT-I.1 mice were backcrossed with $CXCR3^{-/-}$ mice (22) and genotyped to confirm transgene and knockout. Animal treatment was consistent with the National Institutes of Health Guidelines on the Care and Use of Laboratory Animals and all procedures were approved by the University of Oklahoma Health Sciences Center and Dean A. McGee Eye Institute Institutional Animal and Care Use Committee. HSV-1 (strain McKrae) was propagated in green monkey kidney cells (Vero cells), titered, and stored at −80°C as previously described (13).

HSV-1 Infection

Six to ten-week-old male and female WT, gBT-I.1, and gB-$CXCR3^{-/-}$ sex-matched mice were anesthetized by an intraperitoneal (i.p.) injection of xylazine (6.6 mg/kg) and ketamine (100 mg/kg). Their corneas were scarified using a 25 gauge 1 1/2" needle and tear film blotted. 1,000 PFUs of HSV-1 McKrae was resuspended in 3 μLs of sterile 1× PBS and then topically inoculated onto the scarified corneas. HSV-1 viral titers in the cornea were determined 3 and 7 days pi by plaque assay as previously described (13).

Histochemistry

WT and gBT-I.1 mice were infected with HSV-1. Whole eyes were harvested, fixed in 4% paraformaldehyde for 24 hours at 4°C, transferred to 70% ethanol, and embedded in paraffin. 5 μm sections were cut and mounted on slides. Hematoxylin and eosin (H&E) staining was then performed as well as a 1 step trichrome (Gomori's) stain. Uninfected WT and gBT-I.1 mice served as negative controls. Images were then captured using a Nikon Eclipse E800 Epifluorescent microscope (Melville, NY) at 40×, 100×, and 200× magnifications.

Slit Lamp Exam

The corneas of both WT and gBT-I.1 mice were examined 7 days pi for clinical pathology by a "masked" ophthalmologist using a Kowa portable slit lamp (Kowa Optimed Inc., Torrance, CA). Corneal pathology was assessed using the following scoring key: 0 = no pathology; 1 = injected eye, no opacity; 2 = focal opacity; 3 = hazy opacity over entire cornea; 4 = dense opacity in central cornea with remainder hazy; 5 = same as #4 but with ulcer; and 6 = corneal perforation.

ELISAs

At the appointed time, infected gBT-I.1 and WT mice were euthanized and perfused with 1× PBS. Corneas were harvested and resuspended in 1× PBS with a protease cocktail (Calbiochem, La Jolla, CA). Following tissue homogenization, supernatants were clarified with a 10,000 × g spin for 1.5 minutes. Supernatants were then subjected to sandwich ELISAs (R&D Biosystems, Minneapolis, MN) and suspension arrays (BioRad, Hercules, CA) to measure MMP-9, CXCL1, CCL2, CCL5, CXCL9 and CXCL10 levels 7 days pi as previously described (13).

Flow cytometry

Briefly, corneas, draining mandibular lymph nodes (MLNs), and blood [by retroorbital bleed] were harvested from WT and gBT-I.1 mice 0 or 7 days pi. The tissues were then processed to create single cell suspensions by passing through a 40 μm filter that were subsequently labeled with anti-CD8, -CD4, -NK1.1, -CD3, -CXCR3, -CCR5, -CD45 (BD Biosciences, San Jose, CA) and/or tetramer (Baylor College of Medicine, Houston, TX) to identify specific leukocyte populations. The cell suspensions were washed in 1% BSA/PBS and fixed in 1% paraformaldehyde overnight. The samples were then analyzed by flow cytometry (Beckman Coulter, Brea, CA) with known amounts of CountBright beads (Invitrogen, Eugene, OR) as previously described to evaluate total cell numbers found in the respective tissue (13).

Intracellular Staining

Single cell suspensions were isolated as seen above from the draining MLNs of WT and gBT-I.1 mice 7 days pi. 1 million cells were resuspended in 1.0 ml of RPMI 1640 medium containing 10% FBS and added to 24-well culture plates. Cells were stimulated with 2 μg of HSV-specific gB peptide (SSIEFARL) (Biomatik USA, Wilmington, DE) for 1 hour at 37°C at which point 1 μL Brefeldin A (BD Bioscience) was added. After an additional 3 hours at 37°C, nonspecific antibody binding was inhibited with 2 μLs Fc block (BD Bioscience) for 15 minutes at 4°C. Select extracellular receptors were then stained with PE-Cy5-conjugated CD45 and FITC-conjugated CD8 for 30 minutes at 4°C. The cells were permeabilized according to manufacturer's protocol (BD Bioscience). Following permeabilization cells were stained with 4 μLs PE-conjugated IFN-γ (BD Bioscience) at 4°C and twice washed. The single cell suspensions were analyzed by flow cytometry as seen previously.

Confocal Imaging

Corneas were harvested from both WT and gBT-I.1 mice at 0, 7, and 30 days pi. The corneas were fixed in 4% paraformaldehyde and washed in 1% PBS-Triton as previously described (23). The tissue was blocked with Fc block overnight at 4°C and then incubated with primary antibody against CD31 (Millipore) and Lyve 1 (Abcam) overnight at 4°C. Following three washes with 1% PBS-Triton, secondary antibodies were added (Jackson ImmunoResearch Laboratories) and incubated overnight at 4°C. Following three more washes, corneas were incubated at 4°C with Dapi overnight. Corneas were then mounted and imaged as z-stack images using an epifluorescence/confocal laser-scanning microscope (IX81-FV500; Olympus) as previously described (23).

$CD8^+$ T cell depletion

gBT-I.1 transgenic mice were infected with 1,000 PFU / eye HSV-1. After thirty minutes, gBT-I.1 mice were given a subconjunctival injection of either 40 μg of anti-CD8a (Bio X cell, Lebanon, NH) or isotype antibody (rat IgG) resuspended in 10 μls of 1× PBS. The mice were then treated again with 40 μg of antibody at 2, 4, and 6 days pi. At 7 days pi, mice were euthanized and viral content assessed in the cornea by plaque assay as previously described, VEGF isoform expression by RT-PCR, or lymphatic growth by confocal microscopy. Depletion was confirmed by flow cytomeric analysis of the cornea for $CD8^+$ T cell population as previously described.

VEGF-C Neutralization

gBT-I.1 mice were infected as previously described. Three days pi and every-other-day thereafter, mice were given a 10 μl subconjunctival injection (10 μg total) of either human IgG or VEGFR3-Fc (R&D Systems). Lymphatic growth was then evaluated 7 days pi by confocal microscopy as described previously.

RT-PCR

mRNA was isolated from infected and uninfected gBT-I.1 and WT corneas as previously described (24). Briefly, corneas were harvested and homogenized. Total RNA was then isolated using Trizol per manufacturer's guidelines (Invitrogen). cDNA was synthesized using avian myeloblastosis reverse transcriptase and real-time PCR performed with an iCycler. Primer sequences have been previously described (25). To evaluate mRNA expression of trafficking leukocyte populations, MLN and spleen leukocytes were pooled from uninfected and infected mice (day 7 pi) and 1×10^7 cells were subjected to a $CD8^+$ isolation column (Miltenyi Biotec) to isolate $CD8^+$ cells from all others per manufacturer's protocol. RT-PCR was then performed to identify sources of VEGF isoform expression. Flow cytometric analysis was performed to evaluate purity of populations.

Statistics

Statistical analysis was performed using the GBSTAT program (Dynamic Microsystems, Silver Spring, Maryland). A Student's *t* test was used to determine significant ($p < .05$) differences between WT and gBT-I.1 groups.

RESULTS

gBT-I.1 transgenic mice harbor less virus yet have comparable acute corneal pathology to WT animals following ocular HSV-1 infection

$CD4^+$ T cells have been assumed to be the major adaptive leukocyte population driving immune clearance and pathology in the cornea (14, 15). Thus, we sought to evaluate the role, if any, $CD8^+$ T cells have in viral surveillance following ocular HSV-1 infection using transgenic mice in which nearly all of the $CD8^+$ T cells recognize the immunodominant HSV-1 gB peptide epitope (20). To evaluate the role of $CD8^+$ T cells in containing HSV-1 replication, WT and gBT-I.1 mice were ocularly infected with 1,000 PFU and sacrificed either 3 or 7 days post infection (pi). While viral loads were similar 3 days pi (Fig. 1A), infectious virus levels in the cornea of WT mice were 10–100 times higher than gBT-I.1 mice as determined by plaque assay by 7 days pi (Fig. 1B). To next evaluate whether a decreased viral load corresponded with an increase in pathology during the acute infection, we performed H & E staining to identify infiltrating leukocytes, and trichrome staining to visualize collagen fiber destruction/rearrangement. Samples viewed by two masked individuals found no appreciable pathologic differences in the cornea of gBT-I.1 mice and WT counterparts 7 days pi (Fig. 2). Both gBT-I.1 and WT mice had similar presentation of leukocytes residing in the cornea proper (Fig. 2A–B) as well as varying degrees of collagen fiber disruption (Fig. 2E–F) in comparison to WT and gBT-I.1 uninfected controls, which had no measurable leukocyte infiltrate or corneal pathology (Fig. 2C–D, G–H). Clinical slit lamp examination and matrix metalloproteinase-9 (MMP-9) protein levels were consistent with histological specimens in that infected gBT-I.1 mice had only modestly higher clinical scores and similar levels of MMP-9 expression when compared to WT corneas (Fig. 3A–B). Furthermore, infected WT and gBT-I.1 mice showed significantly elevated corneal MMP-9 levels compared to their uninfected counterparts (<.02 ng / mg cornea). To further examine ocular pathology, confocal imaging was performed to evaluate lymphatic and blood vessel growth into the cornea proper. By day 7 pi, both WT and gBT-I.1 mice had lymphatic vessels (yellow arrows, $Lyve1^{hi}$, $CD31^{lo}$) infiltrating the cornea, but only WT mice had appreciable blood vessel genesis ($CD31^+$, $Lyve1^-$) [Fig. 3C–D, **data not shown**]. The lack of blood vessel growth into gBT-I.1 cornea proper was only intensified by day 30 pi compared to WT controls (Fig. 3D, pink arrows). Taken together, gBT-I.1 mice had significantly less virus yet comparable levels of ocular pathology as WT controls during the acute phase of disease (0–7 days pi) suggesting viral loads were not a reliable predictor of

HSK (day 30). These findings also further reiterated a likely immune-mediated role in corneal pathologic outcomes following HSV-1 infection.

HSV-specific CD8$^+$ T cells infiltrate HSV-1 infected corneas of gBT-I.1 mice far in excess of that found in WT controls

In order to identify contributing factors associated with viral surveillance in the cornea of gBT-I.1 mice following HSV-1 infection, leukocyte populations residing in the tissue were phenotypically identified. Whereas the percentage of total CD8$^+$ T cells was not different comparing WT to gBT-I.1 mice (Fig. 4B) there was a substantial difference in the absolute number of HSV-specific CD8$^+$ T cells in the cornea proper with significantly more found in that of gBT-I.1 mice (Fig. 4A and 4C). No other significant differences were found in leukocyte populations (i.e. NK cell [data not shown], CD4$^+$ T cell [Fig. 4D], and total leukocyte influx [Fig. 4E]) within the infected cornea comparing the two groups. Furthermore, this difference in HSV-specific CD8$^+$ T cells was not appreciated 3 days pi due to a lack of CD8$^+$ T cell infiltration (data not shown) and equilibrated by day 30 pi (Fig. 4F).

To determine if the results found in the cornea were reflective of that residing in the draining lymph nodes (mandibular lymph nodes, MLN) to explain the discrepancy in trafficking, select leukocyte populations including NK cells, CD4$^+$ and CD8$^+$ T cells, HSV-specific CD8$^+$ T cells, and total leukocytes were assessed 7 days pi. HSV-1 infected gBT-I.1 mice exhibited gross deficiencies in NK cells (Fig. 5B) and CD4$^+$ T cells (Fig. 5C), yet had significantly more HSV-specific and total CD8$^+$ T cells in the MLN when compared to WT mice (Fig. 5A and 5D). Furthermore, there was a marked increase in the activation of CD8$^+$ T effector cells in response to HSV antigen in the total CD8$^+$ T cell population from the MLN of HSV-1 infected gBT-I.1 mice as determined by IFN-γ expression (Fig. 5E) and less T regulatory cells per effector CD8$^+$ T cell (Fig. 5F). We interpret these results to suggest gBT-I.1 mice are more adept at containing HSV-1 in the cornea due to increased HSV-specific CD8$^+$ T cell numbers that are capable of responding to viral antigen.

Enhanced recruitment of CD8$^+$ T cells into to the cornea of gBT-I.1 mice is associated with an increased expression of chemokine receptor CXCR3

To explain the increased CD8$^+$ T cell trafficking into the cornea of gBT-I.1 mice, chemokine levels of known effector T cell chemoattractants (26–28) as well as inflammatory chemokines were evaluated. T cell chemoattractants including CCL5 and CXCL10 levels were significantly lower in the cornea of gBT-I.1 mice in comparison to WT controls (Fig. 6A). While CXCL9 was lower as well, the difference was not statistically different (Fig. 6A). Likewise, CCL2 but not CXCL1 was elevated in cornea tissue from HSV-1-infected WT mice in comparison to gBT-I.1 transgenic mice (Fig. 6B). Based on these results, chemokine expression parallels antigen load within the cornea of infected mice and does not alone explain the unique recruitment pattern found in the cornea of gBT-I.1 mice. As a result, chemokine receptor expression for the T cell chemoattractants CCL5, CXCL9, and CXCL10 was evaluated on the circulating CD8$^+$ T cell population following HSV-1 infection. The results show a significantly higher proportion of circulating CD8$^+$ T cells from gBT-I.1 mice express CXCR3 but not CCR5 in comparison to that found in WT mice and uninfected controls (Fig. 6C). To further highlight the importance of CXCR3, gBT.I-1 mice were backcrossed with CXCR3 deficient mice (gBT-I.1-CXCR3$^{-/-}$) and infected with HSV-1. gBT-I.1-CXCR3$^{-/-}$ mice had elevated HSV-1 titers in the cornea 7 days pi in comparison to gBT-I.1 controls and was consistent among all three experiments (Fig. 6D). Collectively, these results emphasize the importance of CXCR3 expression on circulating CD8$^+$ T cells in immune surveillance in the cornea.

$CD8^+$ T cells contribute to immune surveillance and lymphatic growth following HSV-1 infection

To substantiate the contribution of $CD8^+$ T cells in gBT-I.1 mouse resistance to HSV-1 infection, $CD8^+$ T cells were depleted (Fig. 7A, 7C). In comparison to isotype control-treated mice, $CD8^+$ T cell-depleted gBT-I.1 mice possessed significantly more infectious virus in the cornea 7 days pi (Fig. 7B). These results substantiate the role of infiltrating $CD8^+$ T cells in immune surveillance of the cornea following ocular HSV-1 infection. To determine if the net loss of virus was correlative with a common pathologic condition of herpetic keratitis, angiogenesis was evaluated 7 days pi in isotype- and $CD8^+$ T cell-depleted corneas (Fig. 7A, 7B). In gBT-I.1 mice depleted of $CD8^+$ T cells, lymphatic length was severely shortened (Fig. 7D), thus suggesting a role of $CD8^+$ T cells in lymphatic growth. From previous work in our lab, acute lymphatic growth was driven in response to VEGF-A production by infected epithelial cells during the first few days pi (25, 29). Thus to identify the discrepancy in lymphatic and blood vessel genesis seen in WT and gBT-I.1 mice following infection (Fig. 3C), mRNA expression was evaluated for VEGF isoforms A, C, and D, known angiogenic factors (30). By day 5 pi, a significant elevation in VEGF-C could be appreciated in gBT-I.1 corneas compared to WT controls (Fig. 8B). Conversely, by day 30 pi WT mice had significantly higher levels of all three isoforms tested than gBT-I.1 corneas (Fig. 8A–C). Previous work has shown that activated T cell lines can be a source of VEGF (31). To identify the role of $CD8^+$ T cells, if any, in lymphatic growth seen in gBT-I.1 mice, mRNA transcripts were evaluated from isolated infected and uninfected WT and gBT-I.1 draining MLNs and spleen (Fig. 8D). In both WT and gBT-I.1 mice, $CD8^+$ T cells were the major source of VEGF-C expression following infection (Fig. 8E). Interestingly, WT $CD8^+$ T cells were also a source of VEGF-A in an infected and uninfected setting (Fig. 8E). To substantiate the role of VEGF-C in lymphatic growth of gBT-I.1 corneas, VEGF-C neutralization was performed and resulted in a severe blunting of lymphatic growth by day 7 pi confirming VEGF-C-dependent lymphatic growth (Fig. 8F).

Discussion

In the present study, an increased influx of $CD8^+$ T cells into the cornea of gBT-I.1 mice following HSV-1 infection was associated with similar acute gross visual pathology with similar NK and $CD4^+$ T cell infiltration profiles and lower viral titers when compared to WT controls. In patients suffering from HSK, HSV-specific $CD8^+$ T cells are found in relative abundance suggesting a role of $CD8^+$ T cells in inducing ocular pathology (32). In fact, mice deficient in $CD4^+$ T cell populations can still develop HSK (33), and the accumulation of activated $CD4^+$ T cells is not sufficient to cause the development of HSK further implicating a non-$CD4^+$ T cell population (34). From the study described herein, $CD8^+$ T cells are not a major contributor to ocular pathology likely due to their ability to efficiently clear virus, thus reducing HSV-driven, VEGF-A-dependent lymphatic growth (25, 29). This is further supported in that a loss or depletion of $CD8^+$ T cells actually leads to enhanced neovascularization, opacity, and scarring (16, 19). However, the few unwarranted effects of these cells within the cornea likely results from the secretion of VEGF isoforms to initiate endothelial migration and proliferation (30). While the secretion of VEGF from T cells has been shown to induce a T_H1 response required to inhibit HSV-1 spread and is likely important in tissues such as the lymph node (13, 31, 35), expression of VEGF in the cornea, more specifically VEGF-C, from $CD8^+$ T cells leads to detrimental lymphatic invasion of the avascular cornea. Lymphangiogenesis has severe visual consequences and is thus, a tightly regulated phenomenon as evident by constitutive expression of soluble VEGFR-1 (36). Our lab had previously reported the importance of VEGF-A in lymphatic growth following HSV-1 infection (25). In the current study, VEGF-A is modestly increased in both WT and gBT-I.1 corneas within the first 24 hours pi. The lower levels of HSV-driven

VEGF-A could be due in part to the lower initial viral inoculum (29). We hypothesize that once VEGF-A has initiated lymphatic growth following HSV infection, VEGF-C then contributes to the vessel lengthening as evidenced by the shorter lymphatic vessels following VEGF-C neutralization compared to IgG controls.

Evidence clarifying the role of immune recognition and clearance of an HSV-1 infection of the cornea is a significant concern to the medical community. With recurrent bouts of herpetic keratitis, the incidence of corneal graft survival following transplantation is severely diminished [>90% (37) to less than 50% (38)] as well as increasing the frequency of corneal blindness due to infectious etiology (1). Thus, a more complete understanding of immune-mediated events following HSV-1 infection could help alleviate the effect the immune response to HSV-1 has on corneal pathology while retaining the host's ability to control the pathogen. Broad-based therapies for HSK such as steroid-based eye drops used to suppress immune responses in the cornea leave the patient modestly immunocompromised (39). This treatment regimen could be supplanted with more specific inhibitors already clinically available for toxic molecules released by activated leukocytes including MMPs, TNF-α, and IFN-γ, all while retaining the host's ability to contain and eventually subdue the infection. Furthermore, adding neutralization of VEGF isoforms with monoclonal antibodies would result in less neovascularization (40) likely resulting in an additive reduction in long-term ocular pathology. Additionally, it is predicted potential vaccines to inhibit HSV infections altogether would require a strong $CD8^+$ T cell activation component to abolish viral-driven VEGF-A production and thus lymphatic growth in the cornea (25, 29). Altogether, a vaccine towards HSV-1 and neutralizing antibodies to VEGF would likely drastically attenuate ocular pathology.

While the increased number of HSV-specific $CD8^+$ T cells in the cornea following infection is not associated with enhanced ocular pathology by clinical examination, the role of HSV-specific $CD8^+$ T cells in viral surveillance and clearance in the cornea should not be underestimated. We had previously described the importance of $CD8^+$ T cells in the CNS following HSV-1 infection (13) and hypothesized these cells were also required in the cornea to contain the virus. In the cornea of gBT-I.1 mice, the increased influx of HSV-specific $CD8^+$ T cells inversely correlated with viral titers 7 days pi despite no other identifiable leukocyte phenotypic difference between gBT-I.1 and WT mice. Moreover, neutralizing $CD8^+$ T cells enhanced gBT-I.1 mouse susceptibility to HSV-1 as seen by an increase in viral titer of $CD8^+$ T cell depleted gBT-I.1 mice. Overall, the results point to a clear role for $CD8^+$ T cells as a contributing cell population in viral surveillance of the cornea.

The unique recruitment of $CD8^+$ T cells in gBT-I.1 mice could not be explained by chemokine production due to deficiencies in T cell chemoattractants CXCL9, CXCL10, and CCL5 production (41–43) compared to WT mice. Thus, circulating gBT-I.1 HSV-specific $CD8^+$ T cells were evaluated for CCR5 and CXCR3 expression. Even though the proportion of $CD8^+$ T cells expressing CXCR3 was significantly higher in gBT-I.1 than WT mice, this may not explain the story in its entirety. Although the importance of CXCR3 in regulating $CD8^+$ T cell trafficking is well described (27, 44), the role of chemokines and their receptors has expanded beyond strict immune trafficking to include functions of activation and immune suppression. CXCR3 has been shown to contribute to $CD8^+$ T cell activation in response to HSV-2 (45) and may initiate similar events in the cornea. While we did not explore the exact deficiency, we speculate that gBT-I.1-$CXCR3^{-/-}$ mice harbored more virus in the cornea than did gBT-I.1 mice due to a loss of $CD8^+$ T cell trafficking and activation. We surmised that since a higher percentage of circulating $CD8^+$ T cells from gBT-I.1 mice expressed CXCR3 than circulating $CD8^+$ T cells from WT mice, the trafficking disparities and potentially increased activity/IFN-γ production of gBT-I.1

leukocytes is, in part, due to this phenomenon. This is supported by previous work in which CXCR3$^{-/-}$ deficient mice have significantly higher viral titers than WT controls 7 days pi in the cornea proper (46). However, another group did not report similar findings (47) indicating the role of CXCR3 in the recruitment of lymphocytes and containment of virus in the cornea remains controversial.

Collectively, the results firmly establish a role for HSV-specific CD8$^+$ T cells in viral containment in the cornea, a role long attributed to CD4$^+$ T cells. Furthermore, the levels of HSV-1 do not correlate with severity of ocular pathology. Thus, the CD8$^+$ T cell immune response to HSV-1 in the cornea contains the virus but does result in a reduction of pathologic outcomes (hemangiogenesis), reiterating the major role of immune-mediated destruction of the cornea following infection. However, CD8$^+$ T cell expression of VEGF isoforms results in lymphatic growth into the cornea proper suggesting some role of CD8$^+$ T cells in lymphangiogensis.

Acknowledgments

The authors would like to thank Sara Moore for technical support and Dr. Carbone for the gBT-I.1 transgenic mice. They would also like to thank Linda Boone and Louisa Williams for their histology expertise and Fatemeh Shariati for genotyping the gBT-I.1 and gBT-I.1-CXCR3$^{-/-}$ transgenic mice (all members of the DMEI CORE lab).

References

1. Xu F, Sternberg MR, Kottiri BJ, McQuillan GM, Lee FK, Nahmias AJ, Berman SM, Markowitz LE. Trends in herpes simplex virus type 1 and type 2 seroprevalence in the United States. JAMA. 2006; 296:964–973. [PubMed: 16926356]
2. Khanna KM, Lepisto AJ, Hendricks RL. Immunity to latent viral infection: many skirmishes but few fatalities. Trends Immunol. 2004; 25:230–234. [PubMed: 15099562]
3. Conrady CD, Drevets DA, Carr DJ. Herpes simplex type I (HSV-1) infection of the nervous system: Is an immune response a good thing? J Neuroimmunol. 2009
4. Carr DJ, Harle P, Gebhardt BM. The immune response to ocular herpes simplex virus type 1 infection. Exp Biol Med (Maywood). 2001; 226:353–366. [PubMed: 11393165]
5. Liesegang TJ. Epidemiology of ocular herpes simplex. Natural history in Rochester, Minn, 1950 through1982. Arch Ophthalmol. 1989; 107:1160–1165. [PubMed: 2757546]
6. Yan XT, Tumpey TM, Kunkel SL, Oakes JE, Lausch RN. Role of MIP-2 in neutrophil migration and tissue injury in the herpes simplex virus-1-infected cornea. Invest Ophthalmol Vis Sci. 1998; 39:1854–1862. [PubMed: 9727408]
7. Duan R, Remeijer L, van Dun JM, Osterhaus AD, Verjans GM. Granulocyte macrophage colony-stimulating factor expression in human herpetic stromal keratitis: implications for the role of neutrophils in HSK. Invest Ophthalmol Vis Sci. 2007; 48:277–284. [PubMed: 17197544]
8. Doymaz MZ, Rouse BT. Herpetic stromal keratitis: an immunopathologic disease mediated by CD4+ T lymphocytes. Invest Ophthalmol Vis Sci. 1992; 33:2165–2173. [PubMed: 1351475]
9. Banerjee K, Biswas PS, Kumaraguru U, Schoenberger SP, Rouse BT. Protective and pathological roles of virus-specific and bystander CD8+ T cells in herpetic stromal keratitis. J Immunol. 2004; 173:7575–7583. [PubMed: 15585885]
10. Koelle DM, Reymond SN, Chen H, Kwok WW, McClurkan C, Gyaltsong T, Petersdorf EW, Rotkis W, Talley AR, Harrison DA. Tegument-specific, virus-reactive CD4 T cells localize to the cornea in herpes simplex virus interstitial keratitis in humans. J Virol. 2000; 74:10930–10938. [PubMed: 11069987]
11. Bonina L, Nash AA, Arena A, Leung KN, Wildy P. T cell-macrophage interaction in arginase-mediated resistance to herpes simplex virus. Virus Res. 1984; 1:501–505. [PubMed: 6335802]
12. Knickelbein JE, Khanna KM, Yee MB, Baty CJ, Kinchington PR, Hendricks RL. Noncytotoxic lytic granule-mediated CD8+ T cell inhibition of HSV-1 reactivation from neuronal latency. Science. 2008; 322:268–271. [PubMed: 18845757]

13. Conrady CD, Thapa M, Wuest T, Carr DJ. Loss of mandibular lymph node integrity is associated with an increase in sensitivity to HSV-1 infection in CD118-deficient mice. J Immunol. 2009; 182:3678–3687. [PubMed: 19265146]

14. Banerjee K, Biswas PS, Rouse BT. Elucidating the protective and pathologic T cell species in the virus-induced corneal immunoinflammatory condition herpetic stromal keratitis. J Leukoc Biol. 2005; 77:24–32. [PubMed: 15496448]

15. Hendricks RL, Tumpey TM. Concurrent regeneration of T lymphocytes and susceptibility to HSV-1 corneal stromal disease. Curr Eye Res. 1991; 10(Suppl):47–53. [PubMed: 1677883]

16. Stuart PM, Summers B, Morris JE, Morrison LA, Leib DA. CD8(+) T cells control corneal disease following ocular infection with herpes simplex virus type 1. J Gen Virol. 2004; 85:2055–2063. [PubMed: 15218191]

17. Nakanishi Y, Lu B, Gerard C, Iwasaki A. CD8(+) T lymphocyte mobilization to virus-infected tissue requires CD4(+) T-cell help. Nature. 2009; 462:510–513. [PubMed: 19898495]

18. Rajasagi NK, Kassim SH, Kollias CM, Zhao X, Chervenak R, Jennings SR. CD4+ T cells are required for the priming of CD8+ T cells following infection with herpes simplex virus type 1. J Virol. 2009; 83:5256–5268. [PubMed: 19279095]

19. Ghiasi H, Cai S, Perng GC, Nesburn AB, Wechsler SL. Both CD4+ and CD8+ T cells are involved in protection against HSV-1 induced corneal scarring. Br J Ophthalmol. 2000; 84:408–412. [PubMed: 10729300]

20. Mueller SN, Heath W, McLain JD, Carbone FR, Jones CM. Characterization of two TCR transgenic mouse lines specific for herpes simplex virus. Immunol Cell Biol. 2002; 80:156–163. [PubMed: 11940116]

21. van Lint A, Ayers M, Brooks AG, Coles RM, Heath WR, Carbone FR. Herpes simplex virus-specific CD8+ T cells can clear established lytic infections from skin and nerves and can partially limit the early spread of virus after cutaneous inoculation. J Immunol. 2004; 172:392–397. [PubMed: 14688347]

22. Wareing MD, Lyon AB, Lu B, Gerard C, Sarawar SR. Chemokine expression during the development and resolution of a pulmonary leukocyte response to influenza A virus infection in mice. J Leukoc Biol. 2004; 76:886–895. [PubMed: 15240757]

23. Conrady CD, Jones H, Zheng M, Carr DJJ. A functional type I interferon pathway drives resistance to cornea herpes simplex virus type 1 infection by recruitment of leukocytes. J Biomed Res. 2011; 25:111–129. [PubMed: 21709805]

24. Conrady CD, Halford WP, Carr DJ. Loss of the type I interferon pathway increases vulnerability of mice to genital herpes simplex virus 2 infection. J Virol. 2011; 85:1625–1633. [PubMed: 21147921]

25. Wuest TR, Carr DJ. VEGF-A expression by HSV-1-infected cells drives corneal lymphangiogenesis. J Exp Med. 2010; 207:101–115. [PubMed: 20026662]

26. Wuest TR, Carr DJ. Dysregulation of CXCR3 signaling due to CXCL10 deficiency impairs the antiviral response to herpes simplex virus 1 infection. J Immunol. 2008; 181:7985–7993. [PubMed: 19017990]

27. Christensen JE, de Lemos C, Moos T, Christensen JP, Thomsen AR. CXCL10 is the key ligand for CXCR3 on CD8+ effector T cells involved in immune surveillance of the lymphocytic choriomeningitis virus-infected central nervous system. J Immunol. 2006; 176:4235–4243. [PubMed: 16547260]

28. Thapa M, Welner RS, Pelayo R, Carr DJ. CXCL9 and CXCL10 expression are critical for control of genital herpes simplex virus type 2 infection through mobilization of HSV-specific CTL and NK cells to the nervous system. J Immunol. 2008; 180:1098–1106. [PubMed: 18178850]

29. Wuest T, Zheng M, Efstathiou S, Halford WP, Carr DJJ. The Herpes Simplex Virus-1 Transactivator Infected Cell Protein-4 Drives VEGF-A Dependent Neovascularization. PLoS Pathog. 2011; 7

30. Olsson AK, Dimberg A, Kreuger J, Claesson-Welsh L. VEGF receptor signalling - in control of vascular function. Nat Rev Mol Cell Biol. 2006; 7:359–371. [PubMed: 16633338]

31. Mor F, Quintana FJ, Cohen IR. Angiogenesis-inflammation cross-talk: vascular endothelial growth factor is secreted by activated T cells and induces Th1 polarization. J Immunol. 2004; 172:4618–4623. [PubMed: 15034080]
32. Maertzdorf J, Verjans GM, Remeijer L, van der Kooi A, Osterhaus AD. Restricted T cell receptor beta-chain variable region protein use by cornea-derived CD4+ and CD8+ herpes simplex virus-specific T cells in patients with herpetic stromal keratitis. J Infect Dis. 2003; 187:550–558. [PubMed: 12599071]
33. Lepisto AJ, Frank GM, Xu M, Stuart PM, Hendricks RL. CD8 T cells mediate transient herpes stromal keratitis in CD4-deficient mice. Invest Ophthalmol Vis Sci. 2006; 47:3400–3409. [PubMed: 16877409]
34. Divito SJ, Hendricks RL. Activated inflammatory infiltrate in HSV-1-infected corneas without herpes stromal keratitis. Invest Ophthalmol Vis Sci. 2008; 49:1488–1495. [PubMed: 18385067]
35. Xu M, Lepisto AJ, Hendricks RL. CD154 signaling regulates the Th1 response to herpes simplex virus-1 and inflammation in infected corneas. J Immunol. 2004; 173:1232–1239. [PubMed: 15240715]
36. Ambati BK, Nozaki M, Singh N, Takeda A, Jani PD, Suthar T, Albuquerque RJ, Richter E, Sakurai E, Newcomb MT, Kleinman ME, Caldwell RB, Lin Q, Ogura Y, Orecchia A, Samuelson DA, Agnew DW, St Leger J, Green WR, Mahasreshti PJ, Curiel DT, Kwan D, Marsh H, Ikeda S, Leiper LJ, Collinson JM, Bogdanovich S, Khurana TS, Shibuya M, Baldwin ME, Ferrara N, Gerber HP, De Falco S, Witta J, Baffi JZ, Raisler BJ, Ambati J. Corneal avascularity is due to soluble VEGF receptor 1. Nature. 2006; 443:993–997. [PubMed: 17051153]
37. Lim L, Pesudovs K, Coster DJ. Penetrating keratoplasty for keratoconus: visual outcome and success. Ophthalmology. 2000; 107:1125–1131. [PubMed: 10857832]
38. Epstein RJ, Seedor JA, Dreizen NG, Stulting RD, Waring GO 3rd, Wilson LA, Cavanagh HD. Penetrating keratoplasty for herpes simplex keratitis and keratoconus. Allograft rejection and survival. Ophthalmology. 1987; 94:935–944. [PubMed: 3309775]
39. Pavan-Langston D, Abelson MB. Glucocorticoid therapy in ocular herpes simplex. II. Advantages. Surv Ophthalmol. 1978; 23:35, 43–37. [PubMed: 568322]
40. Saravia M, Zapata G, Ferraiolo P, Racca L, Berra A. Anti-VEGF monoclonal antibody-induced regression of corneal neovascularization and inflammation in a rabbit model of herpetic stromal keratitis. Graefes Arch Clin Exp Ophthalmol. 2009; 247:1409–1416. [PubMed: 19655160]
41. de Nadai P, Chenivesse C, Gilet J, Porte H, Vorng H, Chang Y, Walls AF, Wallaert B, Tonnel AB, Tsicopoulos A, Zerwes HG. CCR5 usage by CCL5 induces a selective leukocyte recruitment in human skin xenografts in vivo. J Invest Dermatol. 2006; 126:2057–2064. [PubMed: 16778803]
42. Dufour JH, Dziejman M, Liu MT, Leung JH, Lane TE, Luster AD. IFN-gamma-inducible protein 10 (IP-10; CXCL10)-deficient mice reveal a role for IP-10 in effector T cell generation and trafficking. J Immunol. 2002; 168:3195–3204. [PubMed: 11907072]
43. Wendel M, Galani IE, Suri-Payer E, Cerwenka A. Natural killer cell accumulation in tumors is dependent on IFN-gamma and CXCR3 ligands. Cancer Res. 2008; 68:8437–8445. [PubMed: 18922917]
44. Zhang B, Chan YK, Lu B, Diamond MS, Klein RS. CXCR3 mediates region-specific antiviral T cell trafficking within the central nervous system during West Nile virus encephalitis. J Immunol. 2008; 180:2641–2649. [PubMed: 18250476]
45. Thapa M, Carr DJ. CXCR3 deficiency increases susceptibility to genital herpes simplex virus type 2 infection: Uncoupling of CD8+ T-cell effector function but not migration. J Virol. 2009; 83:9486–9501. [PubMed: 19587047]
46. Carr DJ, Wuest T, Ash J. An increase in herpes simplex virus type 1 in the anterior segment of the eye is linked to a deficiency in NK cell infiltration in mice deficient in CXCR3. J Interferon Cytokine Res. 2008; 28:245–251. [PubMed: 18439102]
47. Lundberg P, Openshaw H, Wang M, Yang HJ, Cantin E. Effects of CXCR3 signaling on development of fatal encephalitis and corneal and periocular skin disease in HSV-infected mice are mouse-strain dependent. Invest Ophthalmol Vis Sci. 2007; 48:4162–4170. [PubMed: 17724202]

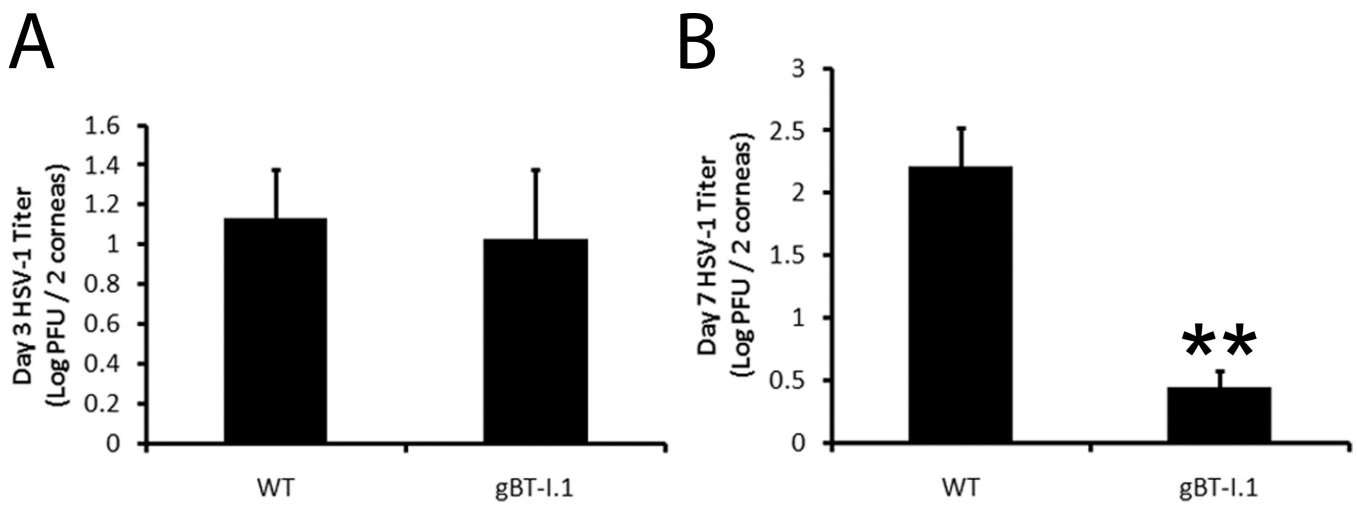

Figure 1. gBT-I.1 mice harbor significantly less virus by day 7 pi than WT controls

WT and gBT-I.1 mice were infected with 1,000 PFU / eye HSV-1. At the indicated time pi, mice were euthanized and corneas harvested. Viral levels in the cornea were evaluated by plaque assay 3 (**A**) and 7 (**B**) days pi. Results represent 2–4 independent experiments of 2–3 mice per group and are expressed as the mean log PFU / cornea ± SEM. **, $p < 0.01$ when comparing gBT-I.1 to WT mice.

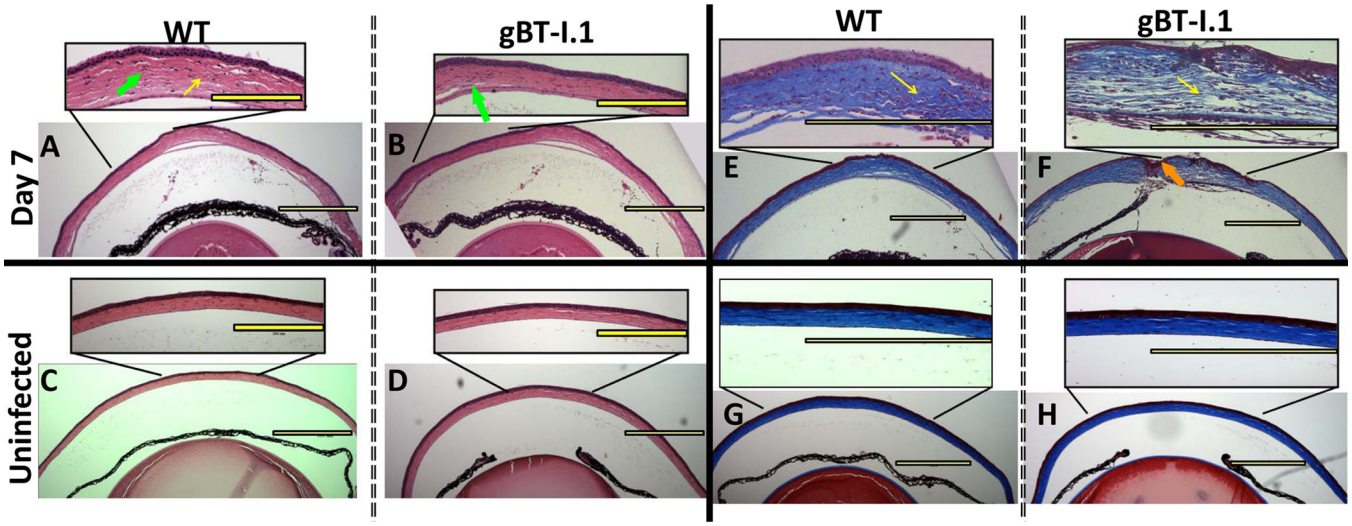

Figure 2. Histological assessment of corneas from HSV-1 infected gBT-I.1 transgenic and WT mice

WT and gBT-I.1 mice were infected with 1,000 PFU / eye HSV-1. Seven days after infection, corneas were harvested, fixed, sectioned and H & E stained to identify generalized leukocyte infiltration (**A–D**) or Gomori's trichrome (**E–H**) stained to evaluate collagen fiber disruption. WT mice (**A**) show leukocytes residing in the cornea proper similar to gBT-I.1 mice (**B**) and collagen fiber disruption as highlighted by the yellow arrow of inset (**E and F**). The orange arrows in (**F**) emphasize sporadic ulcerations more typical of gBT-I.1 mice compared to WT animals. (**C–D; G–H**) are representative images of uninfected controls. All depicted images are representative of 3–4 independent experiments of 2–3 eyes per group. Images are at 40×, 100×, or 400× magnification. Yellow bars, 300 μm.

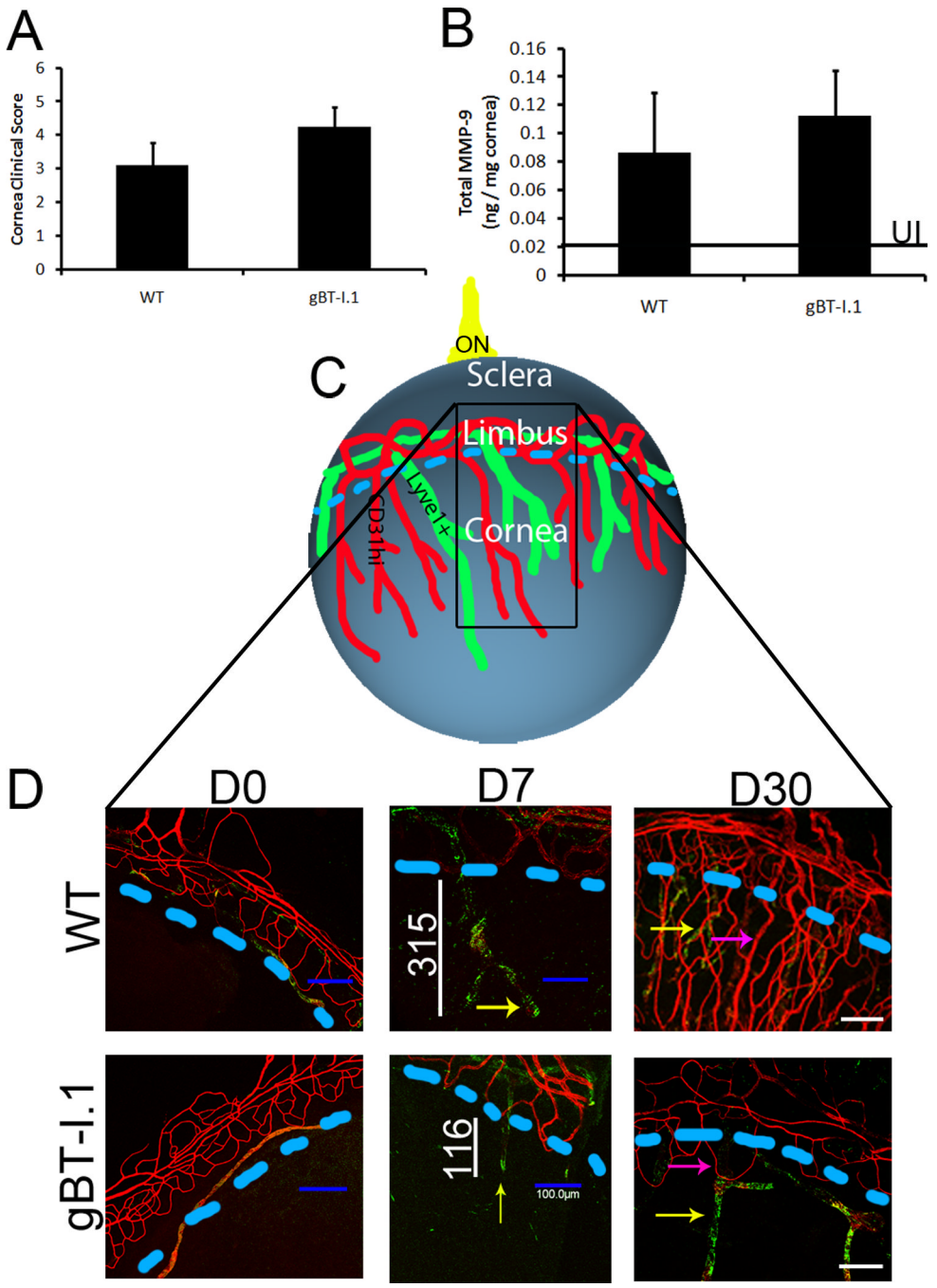

Figure 3. Ocular pathology in WT and gBT-I.1 mouse corneas

WT and gBT-I.1 mice were infected with 1,000 PFU / eye HSV-1 McKrae. At 7 days pi, (**A**) clinical pathology was assessed and scored by a masked observer (clinical ophthalmologist) using a slit lamp exam and no significant differences were identified. (**B**) MMP-9 expression was evaluated by ELISA and were similar in gBT-I.1 and WT mice following infection. Data is represented as the mean ± SEM. Values represent 2 independent experiments of 2–3 mice per group. Black line, MMP-9 expression in uninfected controls. (**C**) An overview of the cornea following HSV infection. Blue line, edge of cornea (limbus region); black box, area imaged; ON, optic nerve. (**D**) Corneas were then assessed for lymphatic (green,

Lyve1^{hi}, CD31^{low}) and blood vessel (red, CD31^{hi}) growth into the cornea proper at 0, 7, and 30 days pi. Pink arrows, blood vessel growth; yellow arrows, lymphatic vessel growth; white lines, length of lymphatic vessel; blue dashed lines, edge of cornea (limbus region).

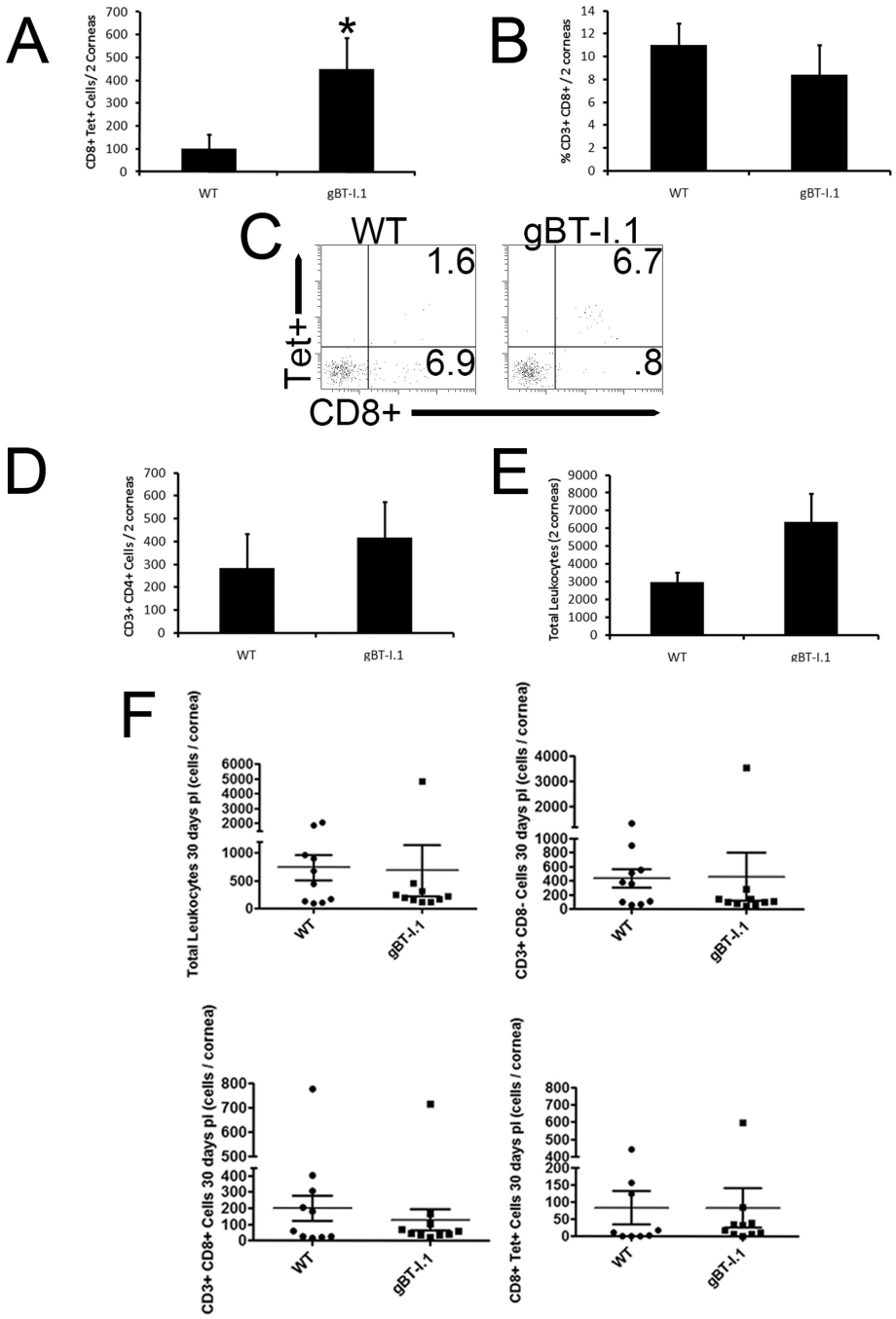

Figure 4. gBT-I.1 mice have a dramatic influx of HSV-specific CD8$^+$ T cells into the cornea not seen in WT

WT and gBT-I.1 mice were infected with 1,000 PFU / eye HSV-1. At 7 or 30 days pi, the animals were ex-sanguinated and the corneas were harvested, processed, and phentotypically characterized for leukocyte content by flow cytometry. Panel (**A**) depicts the HSV-specific CD8$^+$ T cell number 7 days pi. Panel (**B**) shows total CD8$^+$ T cells in the cornea 7 days pi. Panels (**C**) is a representative histogram for the corresponding results reported in panel (**A**). CD4$^+$ T cells and total leukocyte (CD45^{hi}) numbers 7 days pi are expressed in (**D**) and (**E**) respectively. Results from 30 days pi for CD8$^+$ T cells, CD3$^+$ CD8$^-$ cells, HSV-specific CD8$^+$ T cells and total leukocytes are quantified in (**F**). Results in

Panels (**A–B, D–F**) are expressed as the mean ± SEM from 2–3 independent experiments of 2–3 mice per group. *, $p < 0.05$; comparing WT to gBT-I.1.

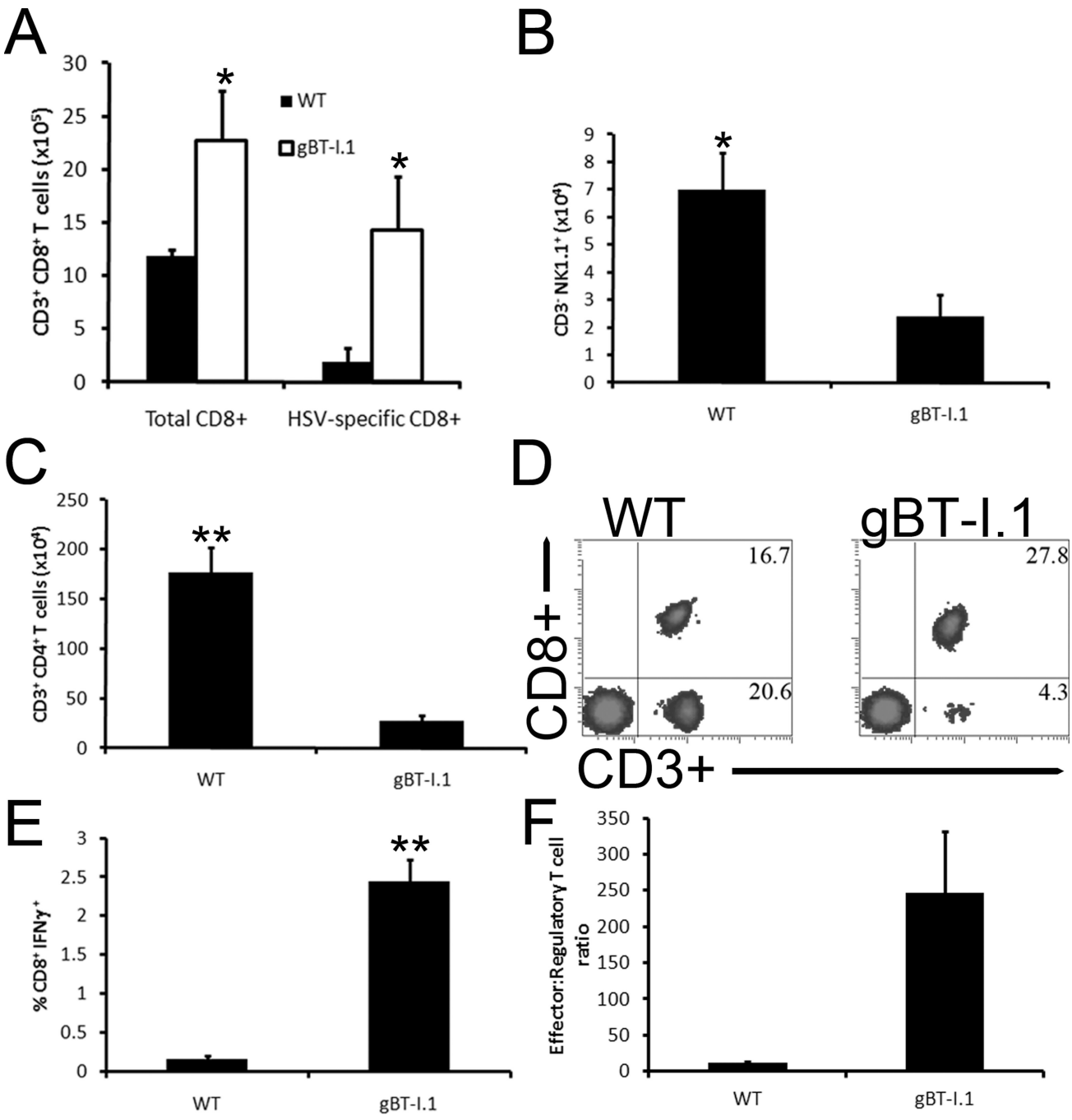

Figure 5. gBT-I.1 mouse draining mandibular lymph nodes possess significantly more total and HSV-specific CD8$^+$ T cells in comparison to WT

WT and gBT-I.1 mice were infected with 1,000 PFU / eye HSV-1. At 7 days pi, leukocytes were isolated from the draining mandibular lymph nodes (MLNs) and phenotypic profiles were analyzed by flow cytometry. gBT-I.1 mouse MLNs contained substantially more HSV-specific and total CD8$^+$ T cells than WT mice (**A**). Conversely, WT mice possessed significantly more CD3$^-$ NK1.1$^+$ (NK cells) and CD3$^+$ CD4$^+$ T cells in the MLN in comparison to gBT-I.1 mice (**B–C**). Representative histograms of flow analysis of CD3$^+$ CD8$^+$ T cells in the MLN is shown in (**D**). gBT-I.1 CD8$^+$ leukocytes were inherently more responsive to HSV-1 than WT cells as indicated by intracellular staining of IFN-γ in (**E**).

Furthermore, gBT-I.1 mice had a higher effector to regulatory T cell ($CD4^+$ $FoxP3^+$) ratio than WT controls (**F**). Results summarize 2–3 experiments of 2–3 mice per group and are depicted as the mean leukocyte population ± SEM. *, $p < 0.05$; **, $p < 0.01$ comparing gBT-I.1 and WT groups.

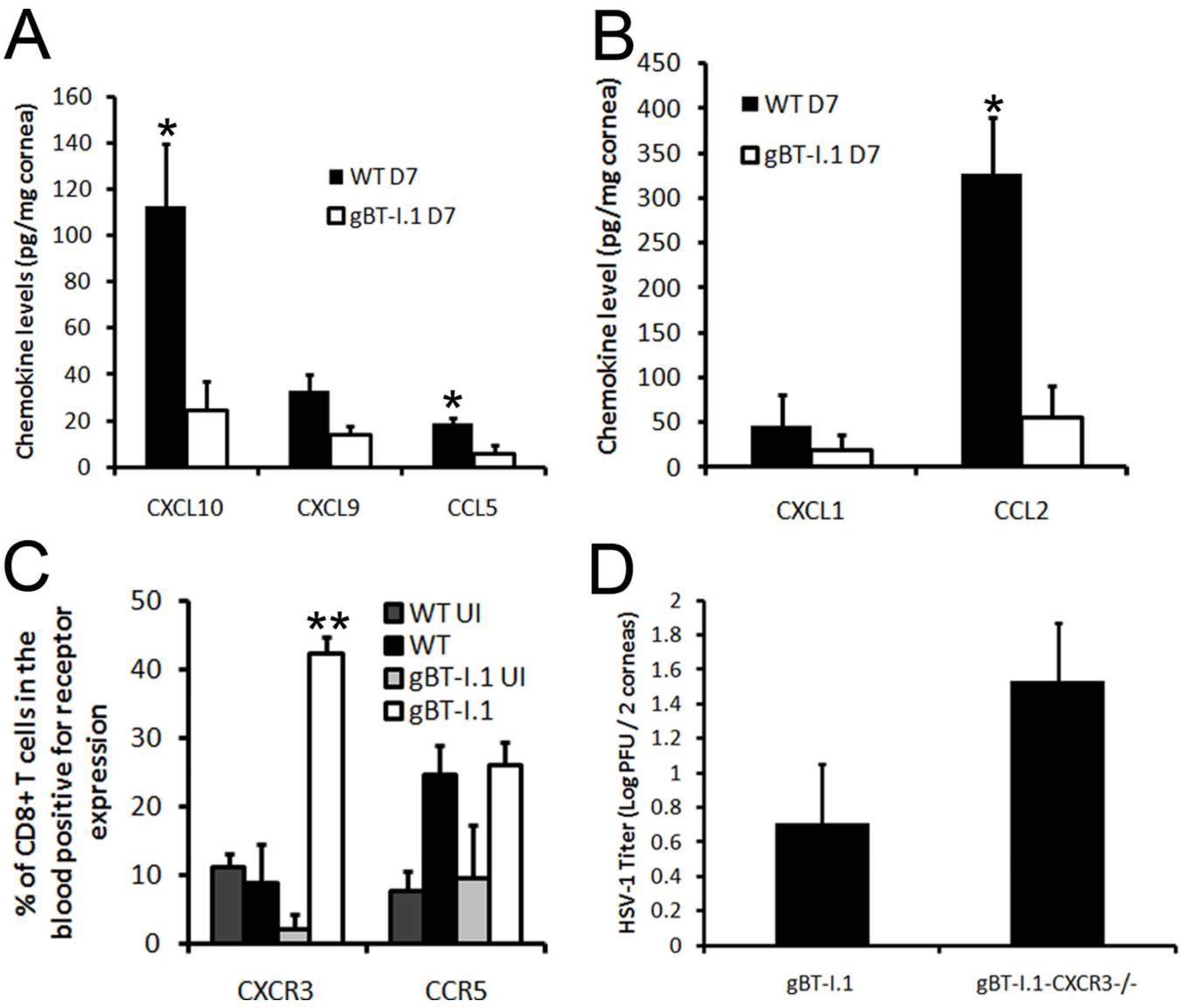

Figure 6. CXCR3 expression is elevated on circulating CD8$^+$ T cells

WT, gBT-I.1, and gB-CXCR3$^{-/-}$ mice (n = 4–6 mice / group) were infected with 1,000 PFU / eye HSV-1. At 0 and 7 days pi, corneas were harvested and assayed for chemokine content by ELISA/suspension arrays. (**A**) WT mouse corneas possessed significantly more CCL5 and CXCL10 compared to gBT-I.1 mouse corneas. (**B**) WT mouse corneas expressed elevated levels of CCL2 but not CXCL1 in comparison to gBT-I.1 mouse corneas. (**C**) CXCR3 but not CCR5 expression is increased on CD8$^+$ T cells obtained from blood samples of gBT-I.1 mice in comparison to infected WT mice. (**D**) gB-CXCR3$^{-/-}$ harbored elevated levels of HSV-1 compared to gBT-I.1 mice as evaluated by plaque assay 7 days pi. Bars represent the mean ± SEM of 2–3 independent experiments. *, $p < 0.05$; $p < 0.01$ when comparing WT to gBT-I.1.

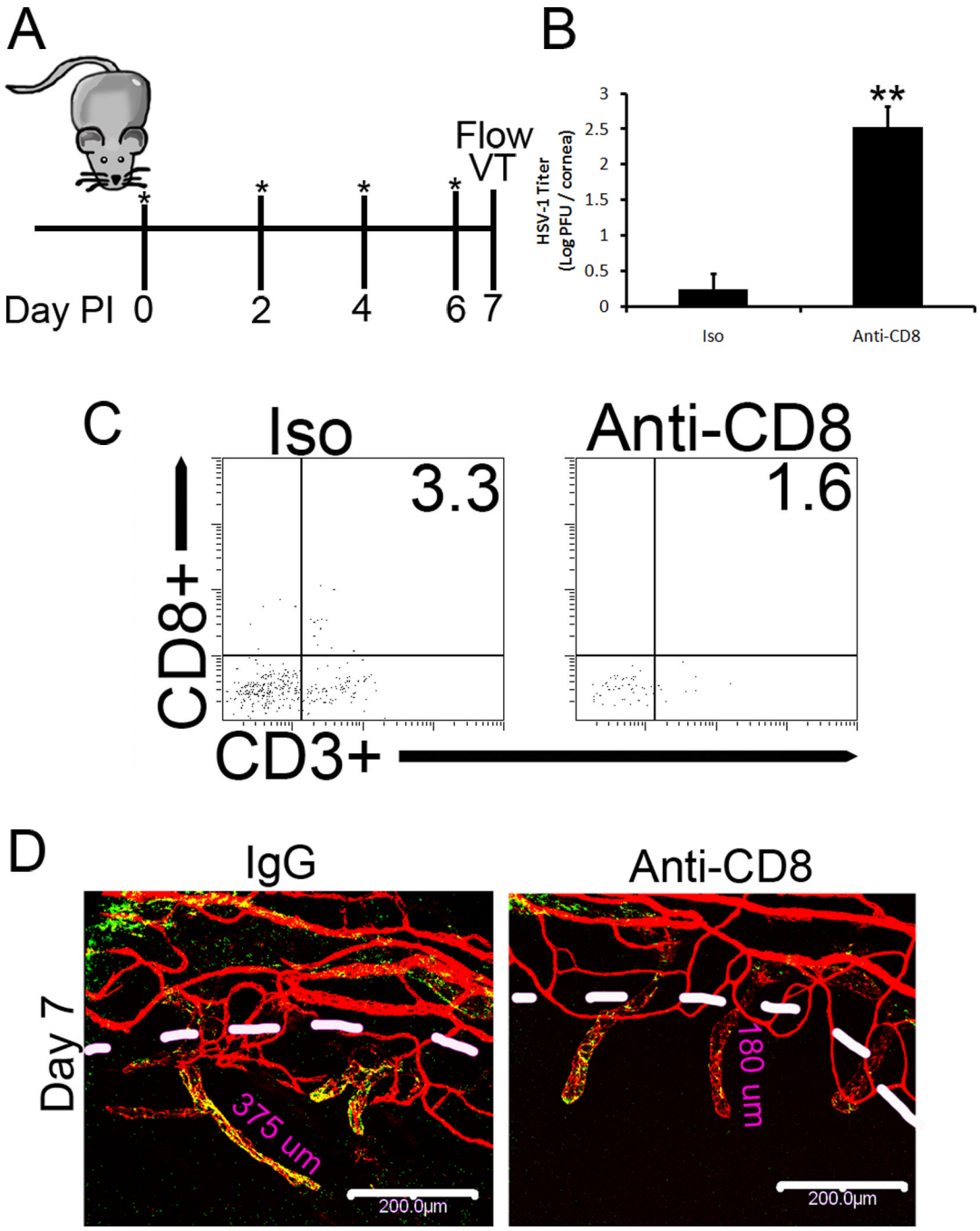

Figure 7. gBT-I.1 mice depleted of CD8$^+$ T cells have significantly higher viral titers in the cornea than isotype-treated gBT-I.1 mice yet shorter lymphatic vessels

gBT-I.1 mice were treated with anti-CD8a or isotype antibody the day of infection and every-other-day thereafter as depicted as asterisks in (**A**). At 7 days pi, corneas were harvested and plaque assay was performed to evaluate infectious virion content (**B**) and flow cytomeric analysis of the cornea (**C**) to confirm CD8$^+$ T cell depletion. Representative histograms following treatment and infection can be seen in (**C**). Values are represented as the mean ± SEM of 2 independent experiments of 2–3 mice / group. (**D**) To investigate the role of CD8$^+$ T cells in angiogenesis, CD8$^+$ T cells were depleted and confocal imaging performed to evaluate lymphatic (green, Lyve1^{hi}, CD31^{lo}) and blood vessel growth (red,

CD31^{hi}). Images are representative of 2 experiments of 2–4 corneas per group. White bars, 200 μm; dashed white lines, border of cornea proper.

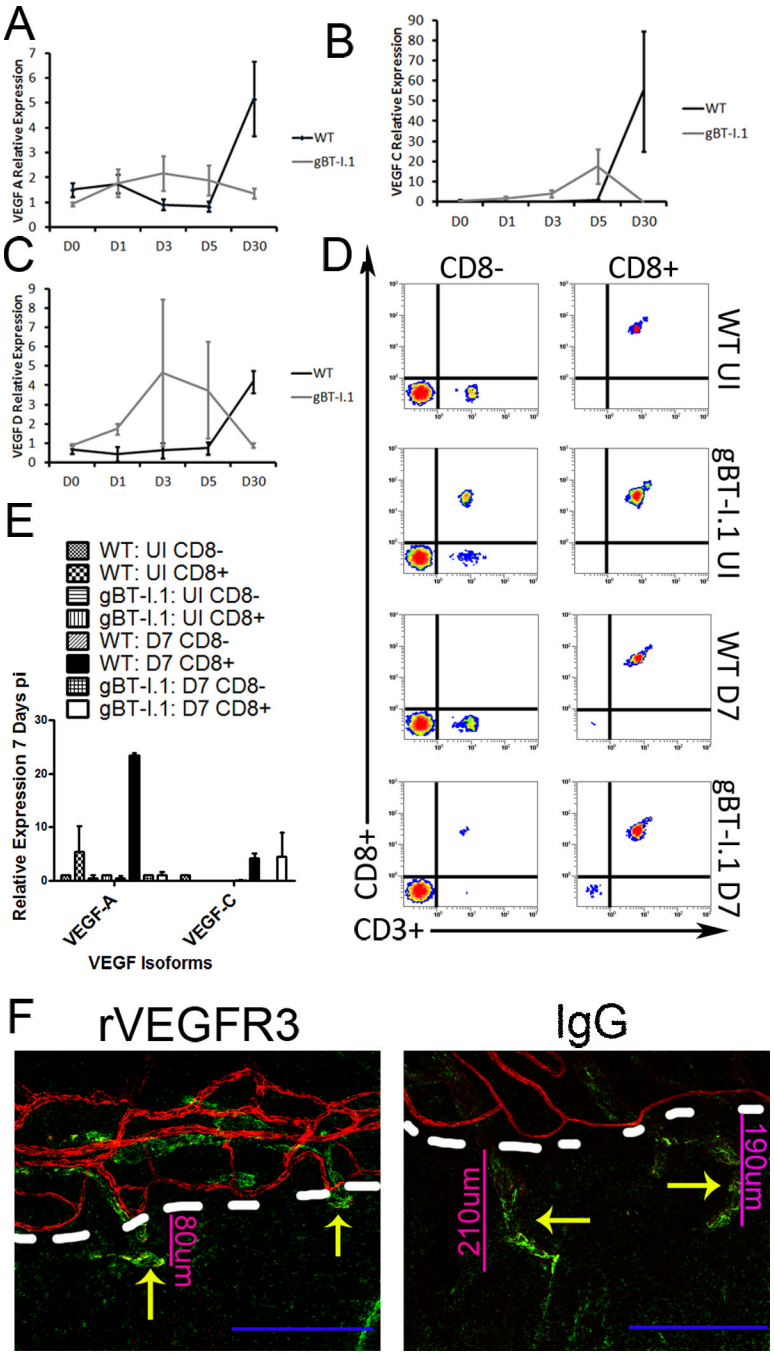

Figure 8. CD8$^+$ T cells secrete VEGF-C to induce lymphatic growth into the cornea

To evaluate the role of CD8+ T cells in lymphangiogenesis, mRNA transcript expression for VEGF-A (**A**), -C (**B**), and -D (**C**) was evaluated 0, 1, 3, 5, or 30 days pi in WT and gBT-I.1 corneas. To then confirm that CD8$^+$ T cells were the major source of VEGF-C, CD8$^+$ and CD8$^-$ cell populations were isolated from the draining MLN and spleen and evaluated for VEGF expression (**E**), and purity evaluated by flow cytometry (**D**). (**E**) To then substantiate the role of VEGF-C in lymphatic growth, chimeric VEGFR3 or control IgG was ocularly administered to gBT-I.1 mice following infection and lymphatic (green Lyve1^{hi}) and blood

vessel (red, CD31^{hi}) growth evaluated by confocal microscopy. Dashed white lines, border of cornea proper with limbus.